Available online at www.sciencedirect.com
SCIENCE DIRECT®
Applied Catalysis A: General 273 (2004) 233–238
APPLIED CATALYSIS A: GENERAL
www.elsevier.com/locate/apcata

Morphology and hydrodesulfurization activity of CoMo sulfide supported on amorphous ZrO_2 nanoparticles combined with Al_2O_3

Guoran Li, Wei Li*, Minghui Zhang, Keyi Tao

Institute of New Catalytic Materials Science, College of Chemistry, Nankai University, Tianjin 300071, China

Received 16 January 2004; received in revised form 17 June 2004; accepted 21 June 2004

Available online 30 July 2004

Abstract

A series of ZrO_2-Al_2O_3 (designated as ZA) mixed supports with different ZrO_2 contents were prepared by a simple complexing-deposition method using $ZrOCl_2 \cdot 8H_2O$ and Al_2O_3 as starting materials. These samples were characterized by inductively coupled plasma–atomic emission spectroscopy (ICP–AES), X-ray diffraction (XRD), N_2 adsorption analysis, X-ray photoelectron spectroscopy (XPS) and transmission electron microscopy (TEM). The results demonstrated that zirconia nanoparticles with a size of about 5 nm in amorphous phase were well dispersed on alumina. The sulfided CoMo catalysts supported on the mixed supports showed a higher dibenzothiophene (DBT) hydrodesulfurization (HDS) activity than those supported on alumina and a commercial HDS catalyst KF757. The NO adsorption analysis revealed that the CoMo/ZA catalysts provided more active sites when the support contained a suitable ZrO_2 content. Further, it was found, by high-resolution transmission electron microscopy (HRTEM), that the addition of ZrO_2 had an obvious effect on the sulfide component's morphology: a multi-layered structure of CoMoS was formed on ZA supports while a mono-layered structure was formed on Al_2O_3. The multi-layered CoMoS on the mixed supports provided more active sites and higher activity for HDS of DBT due to a less steric hindrance.

Keywords: ZrO_2 nanoparticles; Mixed supports; Hydrodesulfurization (HDS); Morphology

1. Introduction

The development of nanoscience makes more opportunities for the innovations of heterogeneous catalysis. For supported catalysts, a new-style catalyst made by substituting nanoscale materials for conventional supports may provide higher catalytic activities; this has attracted increasing attention in recent years [1]. However, a key challenge will be to retain the most active, highest performance physicochemical state of the material even when it is exposed to thermodynamic forces (temperature, pressure, etc.) that would otherwise drive restructuring or agglomeration of the nanoscale material [2]. To meet the challenge, one can prepare a mixed support by means of pinning nanometer-sized particles on a conventional support with high thermal stability; namely, active components of a new-style catalyst are supported on a support modified by nanoparticles.

Hydrodesulfurization (HDS) of feedstock has been an indispensable reaction of producing clean fuels [3–12]. Stringent regulations about gasoline and diesel fuel quality in the near future require improvements in the catalytic performances of HDS catalysts that are conventionally composed of alumina-supported sulfided molybdenum promoted by Co or Ni [3]. As an important method for improving the catalyst, modifying the nature of supports has often been investigated [4–7]. It has been recognized that modifying of the surface of supports may induce variations in dispersion and morphology of active components and possible interactions between metals and supports, which may change the activity and/or selectivity of the catalysts [8]. Unlike TiO_2-Al_2O_3 system that has been studied extensively and thoroughly because of its commercial prospects [9–12], the preparation and the properties of ZrO_2-Al_2O_3 as catalytic supports have not sufficiently been investigated yet, though zirconia-supported molybdenum catalysts have

* Corresponding author. Tel.: +86 22 2350 8662; fax: +86 22 2350 0027.
E-mail address: weili@nankai.edu.cn (W. Li).

0926-860X/$ – see front matter © 2004 Elsevier B.V. All rights reserved.
doi:10.1016/j.apcata.2004.06.038

performed higher intrinsic activity in HDS reactions compared with alumina-supported ones [13]. Mochida and coworkers [6] prepared ZrO_2-Al_2O_3 supports by kneading pseudoboehmite powder and zirconia hydroxide powder with 3.2 % HNO_3, but CoMo/ZrO_2-Al_2O_3 catalyst showed lower activity for HDS of dibenzothiophene (DBT) than CoMo/Al_2O_3. ZrO_2-Al_2O_3 mixed oxides were also prepared by hydrolysis of alkoxides in which zirconium propoxide and aluminum isopropoxide were used, but their catalytic application was not reported [14]. A higher HDS activity of thiophene of CoMo/ZrO_2-Al_2O_3 was reported by the group of Damyanova et al. [15]. It was revealed by X-ray photoelectron spectroscopy (XPS) that the addition of zirconium could promote the dispersion of molybdenum and cobalt species in the oxidic catalysts.

According to our design, ZrO_2 nanoparticles can be dispersedly pinned on Al_2O_3; then active components are loaded to obtain a new-style catalyst. The research results proved that a mixed support composed of amorphous ZrO_2 nanoparticles and Al_2O_3 could be synthesized by a simple complexing-deposition method using $ZrOCl_2{\cdot}8H_2O$ and Al_2O_3 as starting materials. The sulfided CoMo catalysts supported on the mixed oxides provided a higher HDS activity of DBT than CoMo/Al_2O_3 and a commercial catalyst KF757. CoMo/ZA catalysts containing a suitable ZrO_2 content provided more HDS active sites, which was determined by the chemisorption analysis of NO. Further, it was found that more active sites existed in a multi-layer structured morphology on the as-prepared supports compared with the amount in a monolayer on the pure alumina, which was one of the important reasons for the higher catalytic activity.

2. Experimental

2.1. Support and catalyst preparation

The series of ZA supports was designed as ZA*x*, where *x* means the percent by weight of ZrO_2 based on Al_2O_3. The preparation of ZA10 support employed the following procedure: 2.6 g of $ZrOCl_2{\cdot}8H_2O$ was dissolved in 50 ml of the solution of ethanol and deionized water at the volume ratio 1:1. An amount of 3.5 ml of acetylacetone was added to complex ZrO^{2+}, then a glassy yellow solution was obtained when 8.0 ml of ammonium hydroxide was added to adjust pH = ~8.5. 10.0 g of γ-Al_2O_3 obtained by calcination of a commercial pseudoboehmite at 823 K was added to the resultant solution and this mixture was stirred for 3 h at ambient temperature. The mixture was solidified in water bath at 363 K, and then filtered and washed with deionized water. As the final step, the resulting solid was dried at 393 K for 4 h and calcined at 823 K for 4 h in open-air atmosphere. Other mixed supports with various zirconium contents can be prepared by means of changing the amounts of zirconium oxychloride, acetylacetone and ammonium hydroxide proportionally.

CoMo catalysts were prepared using the incipient wetness impregnation method. Supports were impregnated with a mixed aqueous solution of ammonium heptamolybdate tetrahydrate and cobalt nitrate hexahydrate with suitable amounts of ethylenediamine. The samples were dried at 393 K for 4 h and calcined at 573 and 723 K, respectively, for 2 h. The amounts of MoO_3 and CoO in the samples were determined by inductively coupled plasma–atomic emission spectroscopy (ICP–AES). In our case, all the oxidic catalysts contained 17.1 wt.% of MoO_3 and 3.5 wt.% of CoO with 0.1 wt.% of error.

2.2. Characterization

The elemental analysis of the samples was performed by ICP–AES. X-ray diffraction (XRD) patterns of the supports were recorded in the range $5^\circ \leq 2\theta \leq 80^\circ$ in a D/max-2500 diffractometer, using Cu Kα radiation (λ = 1.5418 Å). The specific surface areas, the pore volumes and the pore diameter distributions were measured by N_2 adsorption at 77 K using a Micrometeritics ASAP 2010 apparatus. The measurements of the specific surface areas were performed using a five-point BET method. The BJH method was applied to determine the pore diameter distributions. X-ray photoelectron spectroscopy (XPS) measurements of the supports were performed at room temperature in a Perkin-Elmer PHI (4) 5300ESCA analyzer.

NO adsorption of the sulfided catalysts was carried out in a temperature-programmed desorption (TPD) apparatus. Prior to a conventional TPD process, the samples were in situ presulfided with a mixture of H_2S/H_2 at 673 K. The measurements were focused on the chemical adsorption amounts of NO on the sulfided catalysts.

Transmission electron microscopy (TEM) and high-resolution transmission electron microscopy (HRTEM) observations of the catalysts were made using a TECNAI T20 transmission electron microscope with an acceleration voltage of 200 kV. The sulfided samples were synthesized via the sulfidation of the oxidic precursors under the same conditions as the presulfided process in the activity measurement (see next paragraph). After the sulfided process was completed, the reactor was cooled to room temperature under flowing argon. Then the sulfided catalysts were removed and stored under an argon bottle. The samples for TEM observations were prepared by ultrasonic dispersion in ethanol, and a portion was collected on a holey carbon film mounted on a specimen grid. The specimens were dried naturally in argon atmosphere and rapidly transferred to the analysis chamber in the TEM. At least five representative micrographs were taken for each sample in the high-resolution mode.

2.3. Activity measurement

The HDS reactions of DBT were carried out in a fixed-bed reactor. An amount of 1.0 ml (0.5 g) of oxidic catalysts

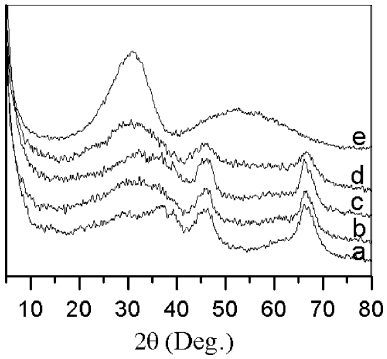

Fig. 1. XRD patterns of: (a) Al_2O_3, (b) ZA05, (c) ZA10, (d) ZA20, and (e) amorphous ZrO_2.

diluted with quartz sand to 5.0 ml were in situ presulfided in a 10 vol% H_2S in H_2 flowing at 30 ml/min at 673 K for 3 h. Then the reactor was cooled to 543 K and then pressurized to 3.0 MPa with H_2. A decalin solution of DBT (0.5 wt.%) was fed into the reactor by a high-pressure pump. The reaction retained a H_2 flow rate of 200 ml/min and a liquid feeding rate of 15 ml/h. The liquid samples were collected at an hour's interval and analyzed by gas chromatography with a flame ionization detector (FID) and a commercial capillary column OV101. The conversion of DBT was used to evaluate the activity of catalysts.

3. Results and discussion

3.1. Characterization of the mixed supports

The XRD patterns of the supports are shown in Fig. 1. It is evident that the Al_2O_3 obtained by calcination of pseudo-boehmite at 823 K is the crystalline γ-Al_2O_3 structure. As compared with Al_2O_3, the mixed oxides ZA05, ZA10 and ZA20 show a broadened peak at $2\theta = \sim 30^\circ$; the intensity of this peak increases with increasing zirconia contents. The broadened peak was attributed to the tetragonal phase zirconia in the literature [14], but it was also considered as an appearance of amorphous zirconia [16]. Here it has been identified by SAED and HRTEM (shown in the later paragraph) that ZrO_2 is amorphous in the ZA supports. The effect of Al_2O_3 in the mixed oxides may be responsible for the existence of the amorphous ZrO_2, though a thermal treatment is carried out at 823 K.

The samples' Zr/Al atomic ratios obtained by ICP and XPS are summarized in Table 1. The results of ICP analysis are in good agreement with the calculated values, but the Zr/Al surface atomic ratios obtained by XPS are ~3 times higher than the corresponding bulk ratios, suggesting that the zirconium oxide is preferentially dispersed on the surface of the alumina.

BET specific surface areas, total pore volumes and average pore diameters of supports have been measured by nitrogen absorption–desorption at liquid nitrogen temperature. The data in Table 1 indicate that the addition of ZrO_2 into the Al_2O_3 support causes a reduction in the surface area and the pore volume of the ZA supports in comparison with the alumina. On the other hand, the average pore diameters of the mixed supports also decrease with increasing ZrO_2 contents, but ZA05 has a larger average pore diameter than Al_2O_3. These results can be attributed to the textual properties of ZrO_2: low surface, small pore volume and dispersed pore distribution [17]. The catalytic supports of hydrotreating catalysts require high specific surface area, large pore volume and wide pore size. The as-synthesized mixed supports respond to the requirement.

The mixed supports were also observed by TEM and HRTEM. Fig. 2 shows a representative TEM image of ZA10. It clearly demonstrates that ZrO_2 nanoparticles with a ~5 nm diameter are well dispersed on Al_2O_3. A higher magnification of this image is presented in Fig. 3. Though the boundary of ZrO_2 particles is blurry due to a small contrast between zirconia and alumina in a HRTEM observation and the rough surface of the supports, we can distinguish the region of ZrO_2 from the micrograph based on its deeper color. It is worthwhile to point out that no lattice spacing is observed in the ZrO_2 nanoparticles [18]; that is, ZrO_2 exists in an amorphous structure, which is also proved by the SAED pattern (the inset in Fig. 3) without any diffraction spot of the crystalline ZrO_2.

3.2. Catalytic activity

DBT HDS activities of the catalysts supported on the as-prepared mixed oxides as a function of ZrO_2 contents based on Al_2O_3 are illustrated in Fig. 4. When 5 wt.% of ZrO_2 is contained in the support (ZA05), the corresponding catalyst performs a higher catalytic activity than the alumina-supported catalyst. Furthermore, a ~10% higher activity is obtained on the catalyst CoMo/ZA10 with the content of

Table 1
Chemical analysis and textural properties of the as-prepared supports

Samples	S_{BET} ($m^2\ g^{-1}$)	Pore volume ($cm^3\ g^{-1}$)	Average pore diameter (nm)	Zr/Al	
				ICP	XPS
Al_2O_3	344.8	1.17	13.6	0	0
ZA05	313.4	1.13	14.3	0.021	0.070
ZA10	303.1	1.00	13.1	0.042	0.132
ZA20	252.8	0.82	12.8	0.083	0.211

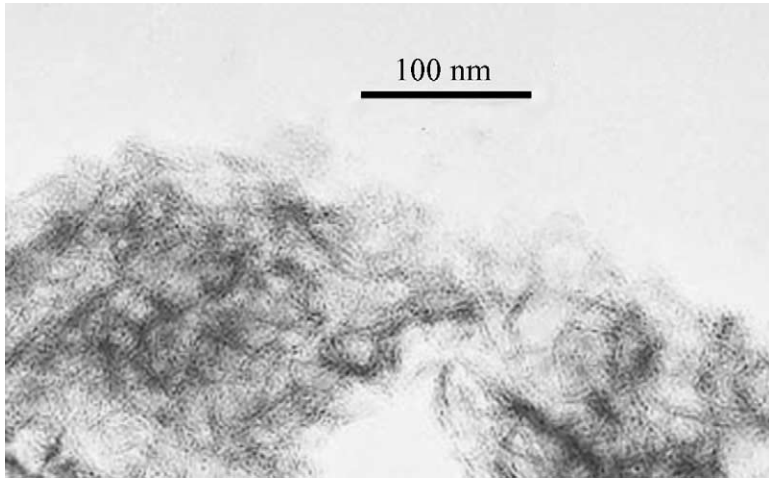

Fig. 2. TEM micrograph of ZA10. The black points mean ZrO_2 particles.

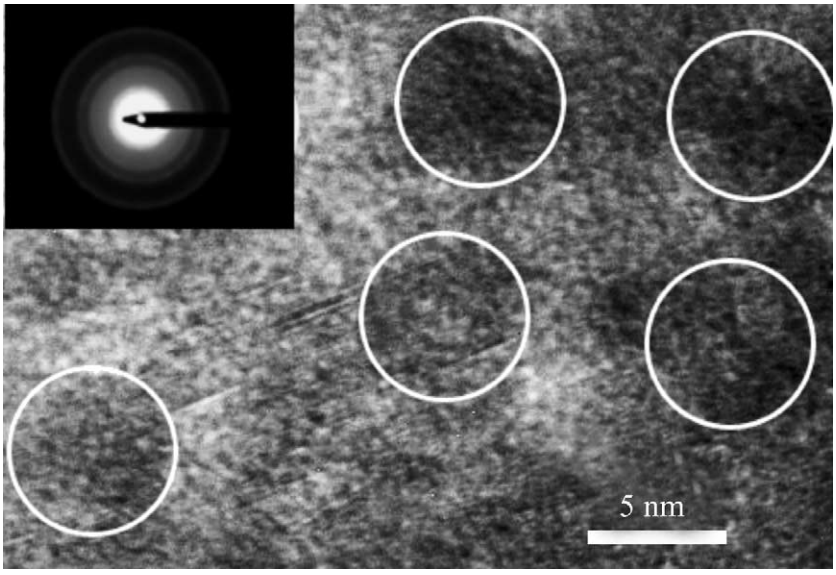

Fig. 3. HRTEM micrograph and SAED pattern (the inset) of ZA10. The circled fields are considered as ZrO_2.

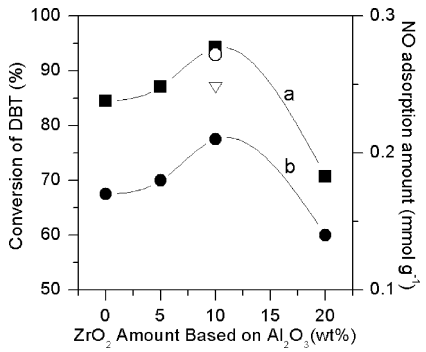

Fig. 4. (a) DBT HDS activities and (b) NO adsorption amounts of sulfided CoMo/ZA as a function of ZrO_2 contents in the mixed supports based on Al_2O_3. The circle (○) and the inverted triangle (▽) are unrelated to the abscissa and denote the catalytic activities of KF757 in the same volume and weight as CoMo/ZA10 catalyst, respectively.

ZrO_2 increasing to 10 wt.%. However, CoMo/ZA20 shows a lower conversion of DBT than $CoMo/Al_2O_3$, which may be related to the poor textural properties of ZA20. These results suggest that the highest DBT HDS activity in this system requires an optimum content of ZrO_2 in the mixed supports, which is 10 wt.% in our research. The circle and the inverted triangle in Fig. 4 denote the catalytic activities of KF757, a commercial HDS catalyst, in the same volume and weight as CoMo/ZA10 catalyst, respectively. CoMo/ZA10 (0.50 g/ml) has a lower loading density than KF757 (0.67 g/ml). It is obvious that CoMo/ZA10 catalyst can provide a higher DBT HDS activity than KF757 under the experimental conditions.

3.3. NO adsorption

The surface structure of oxidic precursors and the nature of the active sites in sulfided $CoMo/Al_2O_3$ and $NiMo/Al_2O_3$

catalysts have been characterized extensively by NO chemisorption by the Topsøe [19] and other groups [20]. These studies demonstrated that NO is a very useful selective probe molecule, and that the number of the active surface sites in activated HDS catalysts can be quantified by NO adsorption. The chemical adsorption amounts of NO on the different catalysts that employed different mixed supports are illustrated in Fig. 4. It is clear that the variation of NO adsorption amounts when ZrO_2 contents increase is consistent with the trend of DBT HDS activity of the catalysts. When ZrO_2 content is 10 wt.%, the corresponding catalyst has the maximum NO adsorption amount.

3.4. TEM observation

Based on the researches in the past several decades, it has been recognized that MoS_2 has slab-like morphologies on supports and that the promoter atoms are located at the edges of the MoS_2 sheets [21]. Further, MoS_2 slabs are basal-bonded or edge-bonded to the support [22], and the morphology and orientation of (Co)MoS_2 will markedly affect the hydrotreating activity of catalysts [21,23]. The sulfided catalysts in our case were observed by a HRTEM. Many black lines appeared in the field of vision of the sulfided catalysts compared with the HRTEM observation of the supports. These black lines could be found in all the fields of the samples, though their dispersions were not very homogeneous. Interestingly, the different forms of the black lines were observed in the different samples. In Figs. 5 and 6, the representative micrographs of CoMo/Al_2O_3 and CoMo/ZA10 are presented, respectively. Some black lines with a 5–8 nm length that were identified to be MoS_2 slabs in many references [21–23] are found in the micrograph of the sulfided CoMo/Al_2O_3, most of which keep clear of each other. This indicates that CoMoS clusters as the active phase exist in a mono-layered morphology on the Al_2O_3. On the other hand, the inspection of Fig. 6 shows that a multi-layered (3–5 layers) morphology of CoMoS with a 5–8 nm length and a ~0.6 nm layer spacing is formed on the ZA10, and that few single black lines can been found. As a result, the alumina-supported sulfided CoMo presents a mono-layered morphology, while most of the ZA10 supported

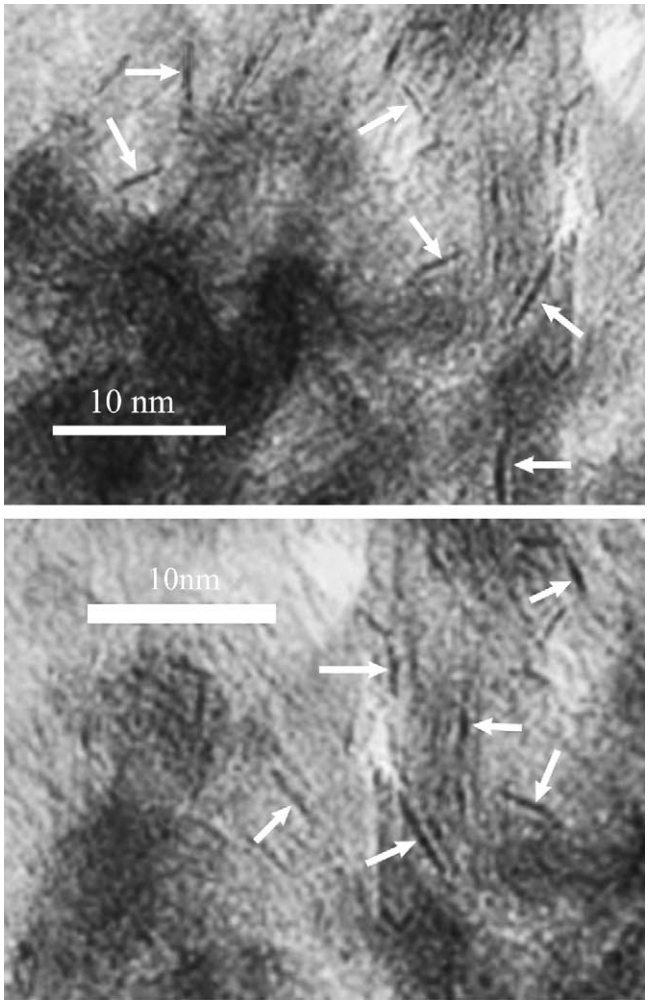

Fig. 5. HRTEM micrographs of the sulfided CoMo/Al showing only mono-layer structured CoMoS clusters.

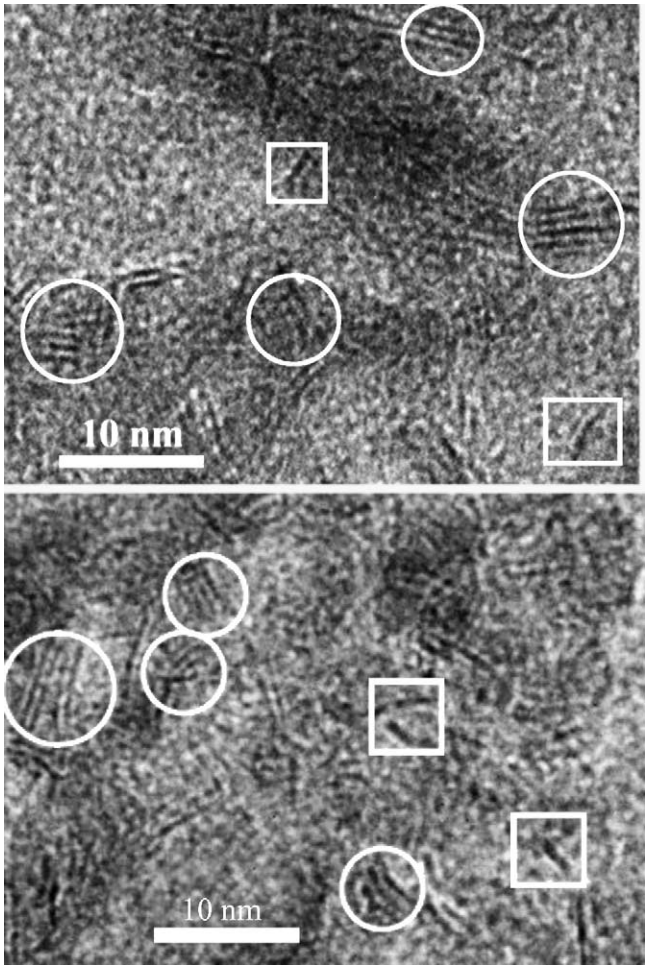

Fig. 6. HRTEM micrographs of the sulfided CoMo/ZA10 showing most multi-layer structured (circles) and some mono-layer structured (square) CoMoS clusters.

ones show a multi-layered structure. The similar phenomena also appeared in the catalysts supported on other mixed supports. As expected, the sulfided CoMo/ZA05 provided less multi-layered structure and more mono-layered structure than CoMo/ZA10, while the sulfided CoMo/ZA20 presented almost the same observed results as CoMo/ZA10.

Shimada and co-workers [22–24] investigated the relation between the catalytic activity of CoMoS structures and the morphology and orientation of MoS_2 clusters on the supports. As a result of the research, the HDS activity decreases in the order of the edge-bonded MoS_2 clusters, the basal-bonded multi-layered MoS_2 clusters and the basal-bonded single-layered MoS_2 clusters, because the upper edge sites of the edge-bonded MoS_2 clusters have less steric hindrance than do the edge sites of the basal-bonded multi-layered MoS_2 clusters, and the edge sites of the basal-bonded multi-layered MoS_2 clusters have less steric hindrance than do edge sites of the bottom layers of the basal-bonded single-layered MoS_2 clusters. In our case, one cannot distinguish between the edge-bonded MoS_2 clusters and the basal-bonded MoS_2 clusters due to the roughness of the support surface. However, a multi-layered MoS_2 structure on the mixed support and a mono-layered structure on the alumina can be respectively observed. The multi-layered CoMoS clusters are responsible for the higher DBT HDS activity, which is consistent with the research result of Shimada and co-workers [22–24].

The morphology of supported MoS_2 depends on the surface properties of the support to a great extent [25]. It is difficult to obtain a direct evidence as to whether the multi-layered sulfided CoMo is only supported on the amorphous ZrO_2 particles or not, but it is obvious that the morphology variation of the CoMoS supported on the mixed oxide is induced by the incorporation of ZrO_2 nanoparticles; namely, the amorphous ZrO_2 is responsible for the formation of the multi-layered CoMoS.

4. Conclusions

ZrO_2-Al_2O_3 (ZA) mixed oxides were prepared by the complexing-deposition method. The special traits of the as-prepared materials were that the amorphous ZrO_2 nanoparticles with a mean size of ~5 nm were well dispersed on the surface of Al_2O_3. As the supports for HDS catalysts, the mixed oxides provided a different morphology of CoMo sulfide due to the effect of the ZrO_2 nanoparticles: a multi-layered structure of the supported sulfided CoMo clusters was formed, as compared with a mono-layered structure of the sulfided CoMo supported on Al_2O_3. This kind of catalysts with the multi-player structured active phase possessed more HDS active sites than the corresponding alumina-supported catalyst, as was measured by NO adsorption. Furthermore, a higher DBT HDS activity could be obtained on the catalysts with the mixed oxides as the supports than on the conventional catalyst. The multi-layered structure of CoMoS should responds to the more active sites and the higher DBT HDS activity due to a less steric hindrance for the adsorption of the reactant molecules.

Acknowledgements

This work was supported, in part, by the National Natural Science Foundation of China (NNSFC) (Grant Nos. 20273035 and 20233030) and by the Natural Science Foundation of Tianjin (NSFT) (Grant No. 033802511).

References

[1] A.T. Bell, Science 299 (2003) 1688.
[2] D.R. Rolison, Science 299 (2003) 1698.
[3] C. Song, X. Ma, Appl. Catal. B 41 (2003) 207.
[4] G.M. Dhar, B.N. Srinivas, M.S. Rana, M. Kumar, S.K. Maity, Catal. Today 86 (2003) 45.
[5] M. Breysse, P. Afanasiev, C. Geantet, M. Vrinat, Catal. Today 86 (2003) 5.
[6] E. Lecrenay, K. Sakanishi, I. Mochida, T. Suzuka, Appl. Catal. A 175 (1998) 237.
[7] C. Flego, V. Arrigoni, M. Ferrari, R. Riva, L. Zanibelli, Catal. Today 65 (2001) 265.
[8] K.C. Pratt, J.V. Sanders, V. Christov, J. Catal. 124 (1990) 416.
[9] E. Olguin, M. Vrinat, L. Cedeno, J. Ramirez, M. Borque, A. Lopez-Agudo, Appl. Catal. A 165 (1997) 1.
[10] S.K. Maity, J. Ancheyta, L. Soberanis, F. Alonso, M.E. Llanos, Appl. Catal. A 244 (2003) 141.
[11] M.P. Borque, A. Lopez-Agudo, E. Olguin, M. Vrinat, L. Cedeno, J. Ramirez, Appl. Catal. A 180 (1999) 53.
[12] S. Damyanova, A. Spojakina, K. Jiratova, Appl. Catal. A 125 (1995) 257.
[13] P. Afanasiev, C. Geantet, M. Breysse, J. Catal. 153 (1995) 17.
[14] T. Klimova, M.L. Rojas, P. Castillo, R. Contreras, J. Ramirez, Microporous Mesoporous Mater. 20 (1998) 293.
[15] S. Damyanova, L. Petrov, P. Grange, Appl. Catal. A 239 (2003) 241.
[16] S. Damyanova, P. Grange, B. Delmony, J. Catal. 168 (1997) 421.
[17] A.B. Gaspar, L.C. Dieguez, J. Catal. 220 (2003) 309.
[18] M.A. Schofield, C.R. Aita, P.M. Rice, M. Gajdardziska-Josifovska, Thin Solid Films 326 (1998) 106.
[19] N.Y. Topsøe, H. Topsøe, J. Catal. 84 (1983) 286.
[20] M. Yamada, N. Koizumi, M. Yamazki, Catal. Today 50 (1999) 3.
[21] E.J.M. Hensen, P.J. Kooyman, Y. van der Meer, A.M. van der Kraan, V.H.J. de Beer, J.A.R. van Veen, R.A. van Santen, J. Catal. 199 (2001) 224.
[22] Y. Sakashita, Y. Araki, K. Honna, H. Shimada, Appl. Catal. A 197 (2000) 247.
[23] Y. Araki, K. Honna, H. Shimada, J. Catal. 207 (2002) 361.
[24] H. Shimada, Catal. Today 86 (2003) 17.
[25] Y. Sakashita, Surf. Sci. 489 (2001) 45.